Mechanisms of Bed Agglomeration During Fluidized-Bed Combustion of Biomass Fuels

ARTICLE *in* ENERGY & FUELS · APRIL 2005

Impact Factor: 2.79 · DOI: 10.1021/ef0400868

3 AUTHORS, INCLUDING:

Marcus Öhman
Luleå University of Technology
86 PUBLICATIONS **1,987** CITATIONS
SEE PROFILE

Anders Nordin
Umeå University
66 PUBLICATIONS **1,713** CITATIONS
SEE PROFILE

Article

Mechanisms of Bed Agglomeration during Fluidized-Bed Combustion of Biomass Fuels

Elisabet Brus, Marcus hman, and Anders Nordin

Energy Fuels, **2005**, 19 (3), 825-832• DOI: 10.1021/ef0400868 • Publication Date (Web): 30 April 2005

Mechanisms of Bed Agglomeration during Fluidized-Bed Combustion of Biomass Fuels

Elisabet Brus, Marcus Öhman,* and Anders Nordin

Energy Technology and Thermal Process Chemistry, Umeå University, S-901 87 Umeå, Sweden

Received September 14, 2004. Revised Manuscript Received February 23, 2005

The major ash-related problem encountered in fluidized beds is bed agglomeration, which, in the worst case, may result in total defluidization of the bed and unscheduled downtime. Because of the special ash-forming constituents of biomass fuels, several of these fuels have been shown to be especially problematic. Despite the frequent reporting, a precise and quantitative knowledge of the bed agglomeration process during fluidized bed combustion of biomass fuels has not yet been presented. Bed sampling versus operation time was performed in four different biomass-fired full-scale fluidized beds, as well as during controlled fluidized bed agglomeration tests in bench-scale testing of five representative biomass fuels. The bed materials and agglomerates were further analyzed using scanning electron microscopy, coupled with energy-dispersive spectroscopy (SEM/EDS), to determine the characteristics of the formed bed particle layers. For typical wood fuels, coating-induced agglomeration with subsequent attack (reaction) and diffusion by calcium into the quartz was identified to be the dominating bed agglomeration mechanism. Low-melting calcium-based silicates (including minor amounts of, for example, potassium) were formed with subsequent viscous-flow sintering and agglomeration. For high-alkali-containing biomass fuels, direct attack of the quartz bed particle by potassium compounds in a gas or aerosol phase formed a layer of low-melting potassium silicate. Thus, formation and subsequent viscous-flow sintering and agglomeration seemed to be the dominating agglomeration mechanism for these fuels.

Introduction

The agglomeration of bed material may cause significant operating problems during fluidized-bed combustion (FBC). In the most-severe cases, it can lead to total defluidization, resulting in an unscheduled plant shutdown. Because of the varying characteristics, and the reactive and most often fluxing nature of ash-forming elements in biomass fuels, many of these fuels have been shown to enhance agglomeration during FBC. Although this has been recognized for decades and literally hundreds of papers that involve the agglomeration problem can be found in the literature, the responsible mechanisms are far from being elucidated.

The state-of-the-art of bed agglomeration mechanisms was recently compiled by Brus in an extensive literature review.[1] The review revealed that many reports very early suggested liquid-phase (melt) formation as a responsible mechanism for sintering, bed agglomeration, and bed defluidization. The melting behavior seems to control the adhesive forces, which are responsible for the temperature-controlled agglomeration process. Melts of both salt[2−5] and silicate[6−10] types have been reported. Chemical reaction sintering[11] and occasionally solid-state sintering[12] have also been used to explain layer formation, sintering, and agglomeration.

Agglomeration has also been suggested to proceed sequentially by initial coating formation (coating-induced agglomeration)[13,14] but also via some type of assumptions of attack of, or reaction with, the quartz bed particles by ash constituents.[15−17] The initial coating formation is then followed by subsequent adhesion and

*Author to whom correspondence should be addressed. Phone:+ 46 90 7866324. Fax:+ 46 90 7869195. E-mail address: marcus.ohman@chem.umu.se.

(1) Brus, E. Licentiate Thesis, Umeå University, 2004, pp 1−37. (ISBN 91-7305-676-6.)

(2) Manzoori, A. R.; Agarwal, P. K. *Fuel* **1992**, *71*, 513−522.

(3) Vuthaluru, H. B.; Zhang, D.-K.; Linjewile, T. M. *Fuel Process Technol.* **2000**, *67*, 165−176.

(4) Davis, C. E.; Dawson, G. B.; Fieldes, R. B. *Fluidization VI: Proceedings of the International Conference on Fluidization*; Grace, J. R., Shemilt, L. W., Bergounou, M. A., Eds; The Engineering Foundation: New York, 1989; pp 555−562.

(5) Nordin, A.; Öhman, M.; Skrifvars, B.-J.; Hupa, M. *Proc. Eng. Found. Conf.* **1995**, 353−366.

(6) Dawson, M. R.; Brown, R. C. *Fuel* **1992**, *71*, 585−592.

(7) Ergudenler, A.; Ghaly, A. E. *Biomass Bioenergy* **1993**, *4*, 135−147.

(8) Skrifvars, B.-J.; Sfiris, G.; Backman, R.; Widegren-Dafgård, K.; Hupa, M. *Energy Fuels* **1997**, *11*, 843−848.

(9) Brus, E.; Öhman, M.; Nordin, A.; Skrifvars, B.-J.; Backman, R. *IFRF Combustion Journal*; International Flame Research Foundation: Ottawa, Canada, 2003; Article Number 200302, pp 1−12. (Electronic publication, ISSN 1562−479X.)

(10) Nuutinen, L. H.; Tiainen, M. S.; Virtanen, M. E.; Enestam, S. H.; Laitinen, R. S. *Energy Fuels* **2004**, *18*, 127−139.

(11) Skrifvars, B.-J.; Hupa, M.; Anthony, E. J. *Proc. Int. Conf. Fluid Bed Combust.* **1997**, *14th*, 819−829.

(12) Anthony, E. J.; Iribarne, A. P.; Iribarne, J. V. *Proc. Int. Conf. Fluid Bed Combust.* **1995**, *13th*, 523−533.

(13) Visser, H. J. M.; van Lith, S.; Kiel, J. H. A. In *Proceedings: 12th European Conference on Biomass for Energy, Industry and Climate Protection,* Amersterdam, The Netherlands, June 2002; Vol. 1, pp 585−588.

(14) Öhman, M.; Nordin, A.; Skrifvars, B.-J.; Backman, R.; Hupa, M. *Energy Fuels* **2000**, *14*, 169−178.

10.1021/ef0400868 CCC: $30.25
Published on Web 04/30/2005

Table 1. Summary of the Bed Material and Operational Data for the Sampling Campaign

plant	abbreviation	bed mass (ton)	bed mtrl consumption (wt % of bed/day)	bed particle size (μm)	bed temp (°C)	fuel	campaign duration (days)
Skellefteå Kraft CFB 90 MW_{th}	CFB90	20	10	200−500	780−850	100% sawdust	17
Brista Kraft CFB 122 MW_{th}	CFB122	20−25	50	280	840−880	40% bark, 60% sawdust + logging debris	21
C-4 Energi BFB 50 MW_{th}	BFB50	30	10	700	790−850	90% logging debris, 10% sawdust	14
Falu Energi BFB 30 MW_{th}	BFB30	20	<3	700	800−880	10% bark, 30% logging debris, 40% wood chips	33 (175)

Table 2. Fuel Characteristics, as Well as Main- and Ash-Forming Elements

	Bench Scale					Full Scale			
	bark	reed canary grass	peat	olive residues	straw	CFB 90	CFB 122	BFB 50	BFB 30
dry substance (wt %)	90.6	90.5	89.1	85.6	90.3	n.a.[a]	n.a.[a]	n.a.[a]	n.a.[a]
ash (wt % of dry substance)	3.0	5.7	2.4	9.9	5.9	1.0	2.9	2.3	1.6
C (wt % of dry substance)	51.6	46.5	53.6	50.2	44.8	n.a.[a]	n.a.[a]	n.a.[a]	n.a.[a]
H (wt % of dry substance)	6.0	5.7	6.2	6.3	0.8	n.a.[a]	n.a.[a]	n.a.[a]	n.a.[a]
O (wt % of dry substance)	39.3	41.6	31.2	32.1	42.6	n.a.[a]	n.a.[a]	n.a.[a]	n.a.[a]
N (wt % of dry substance)	<0.1	0.4	3.2	1.4	0.8	n.a.[a]	n.a.[a]	n.a.[a]	n.a.[a]
Cl (wt % of ash content)	0.3	0.5	0.4	1.5	4.9	<1	0.4	0.9	<0.6
S (wt % of ash content)	1.0	1.8	4.2	1.4	2.9	1.3	1.2	2.5	1.4
SiO_2 (wt % of ash content)	15	77	22	36	39	7.8	15	23	16
Al_2O_3 (wt % of ash content)	2.2	1.4	6.3	3.6	0.71	2.9	2.7	3.1	2.2
Fe_2O_3 (wt % of ash content)	<3.9	0.85	28	4.3	0.52	1.6	1.7	12	11
CaO (wt % of ash content)	39	5.5	24	18	9.7	41	38	34	38
MgO (wt % of ash content)	3.9	1.3	1.4	12	2.9	5.3	3.6	4.6	4.1
Na_2O (wt % of ash content)	<1.6	1.2	1.1	1.7	0.82	0.091	0.74	1.6	0.85
K_2O (wt % of ash content)	7.7	3.6	2.5	18	25	9.1	7.5	9.3	7.9
MnO_2 (wt % of ash content)	1.4	0.2	0.80	n.a.[a]	0.062	n.a.[a]	n.a.[a]	n.a.[a]	n.a.[a]
P_2O_5 (wt % of ash content)	2.8	2.1	2.3	4.0	5.8	4.3	3.4	5.0	3.8
TiO_2 (wt % of ash content)	0.88	0.060	0.27	n.a.[a]	0.05	n.a.[a]	n.a.[a]	n.a.[a]	n.a.[a]

[a] Not analyzed.

agglomeration. From previous extensive studies,[13,14,18] there are strong indications that the coating layers formed on the bed particles during combustion have an important role in the agglomeration process, and it is suggested that coating-induced agglomeration is the main route for agglomeration/defluidization during the FBC of biomass fuels. If this coating consists of compounds with low melting temperatures (melts) and high viscosity, it will evidently result in agglomeration of the bed material.[19,20] The coatings have also been reported to contain several superimposed layers;[10,21] however, their characteristics, formation mechanisms, and roles in the agglomeration process have not yet been fully determined.

The deposition of fine (<5 μm) particles[15] and/or condensation of volatile alkali species[22] have been indicated as critical transport mechanisms to the surfaces of the bed particles. On the other hand, several

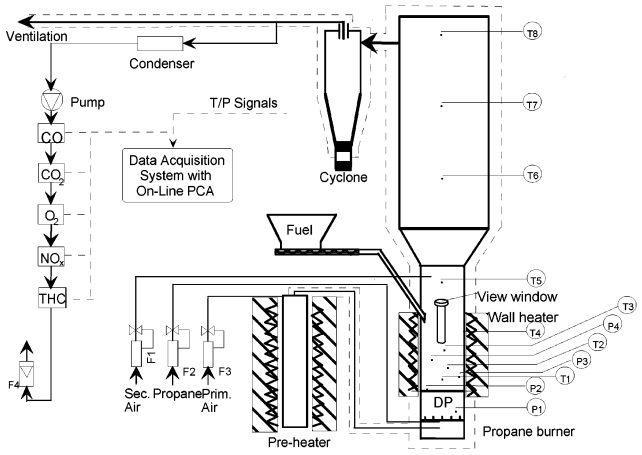

Figure 1. Illustration of the bench-scale fluidized bed reactor for controlled fluidized-bed agglomeration (CFBA) tests (P1−P4, differential bed pressures; T1−T8, thermocouples; F1−F3, mass-flow controllers; and DP, distributor plate).

others suggested the importance of melted ash, either as freely moving particles/droplets or on char particles, transporting this material to bed particle coatings via collisions.[20,23] A few authors reported a layer growth that was only slightly related to the temperature; therefore, they suggested physical processes rather than melts and chemical reactions as a reason for the ash deposition.[20,24,25] Because a liquid was not observed in these studies and the attachment was not accompanied by a sticky layer, only the smallest particles adhered.

(15) Latva-Somppi, J.; Kurkela, J.; Tapper, U.; Kauppinen, E. I.; Jokiniemi, J. K.; Johanson, B. *Proceedings: International Conference on Ash Behavior Control in Energy Conversion Systems*, Yokohoma, Japan, March 1998; pp 119−126.
(16) Brus, E.; Öhman, M.; Nordin, A.; Boström, D.; Hedman, H.; Eklund, A. *Energy Fuels* **2004**, *18*, 1187−1193.
(17) Lind, T. Ash Formation in Circulating Fluidised Bed Combustion of Coal and Solid Biomass; Ph.D. Dissertation; *VTT Publication 378*; Technical Research Centre of Finland: Espoo, Finland, 1999; pp 1−166. (ISBN 951-38-5365-9.)
(18) Benson, S. A.; Karner, F. R.; Goblirsch, G. M.; Brekke, D. W. *Prepr. Pap.—Am. Chem. Soc., Div. Fuel Chem.* **1982**, *27*, 174−181.
(19) Lin, W.; Krusholm, G.; Dam-Johansen, K.; Musahl, E.; Bank, L. *Proc. Int. Conf. Fluid Bed Combust.* **1997**, *14th*, 831−837.
(20) Manzoori, A. R.; Agarwal, P. K. *Fuel* **1994**, *73*, 563−568.
(21) Daavitsainen, J. H. A.; Nuutinen, L. H.; Ollila, H. J.; Tiainen, M. S.; Virtanen, M. E.; Laitinen, R. S. *Proc. Int. Conf. Fluid. Bed Combust.* **2001**, *16th*, 1541−1549.
(22) Mann, M. D.; Galbreath, K. C.; Kalmanovitch, D. P. *Proc. Eng. Found Conf.* **1992**, 773−789.
(23) Lin, W.; Dam-Johansen, K.; Frandsen, F. *Chem. Eng. J.* **2003**, *96*, 171−185.
(24) Manzoori, A. R.; Agarwal, P. K. *Fuel* **1993**, *72*, 1069−1075.

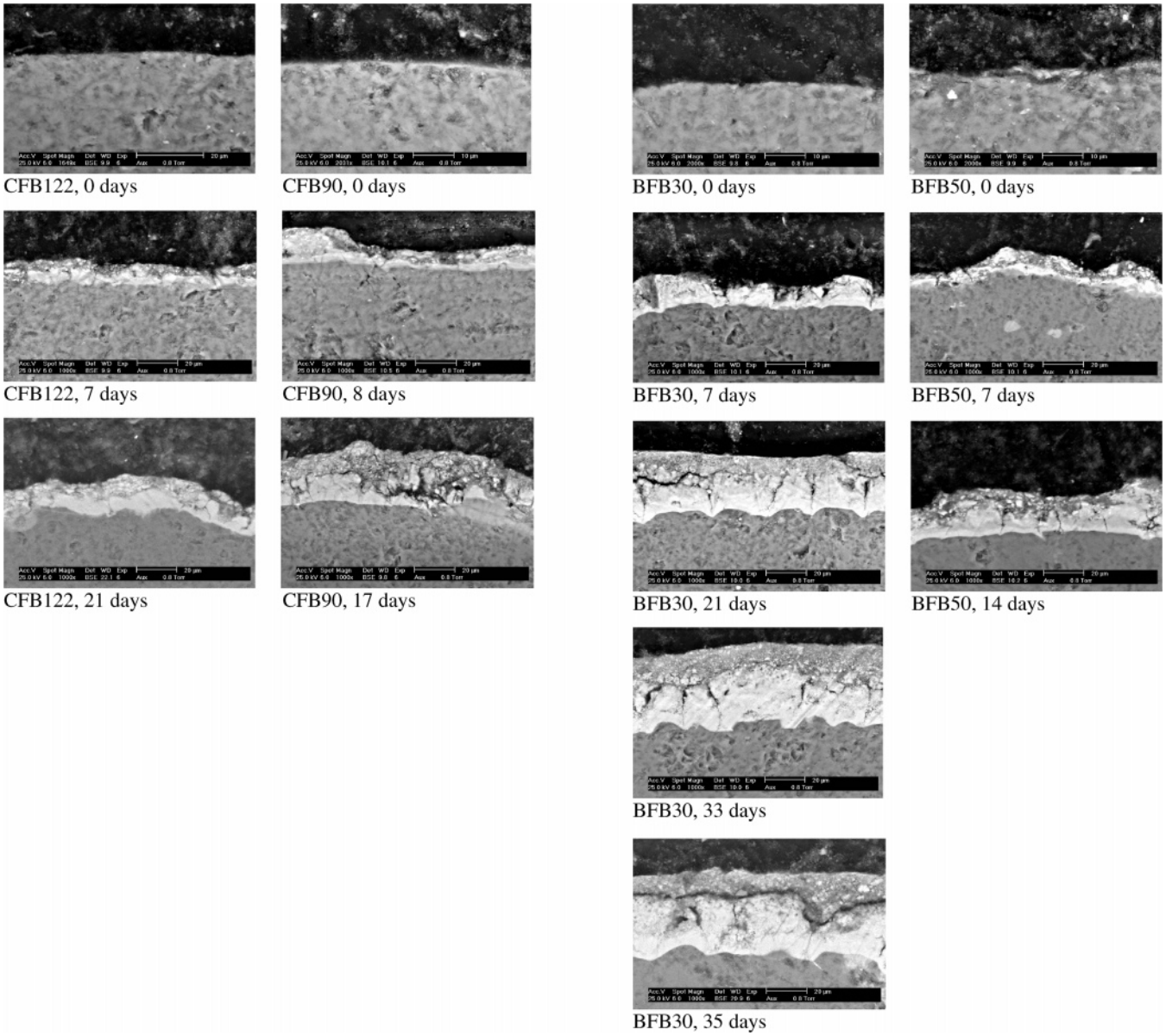

Figure 2. Scanning electron microscopy (SEM) images of typical cross sections of bed particle layers as a function of time: (a) circulating fluidized bed (CFB) material and (b) bubbling fluidized bed (BFB) material. In panel a, material CFB122 is represented in the images on the left, whereas material CFB90 is represented in the images on the right. In panel b, material BFB30 is represented in the images on the left and material BFB50 is represented in the images on the right.

Surface forces (e.g., van der Waals or electrostatic forces) were thereafter attributed to the adhesion mechanism.[25] After the particles were attached on the sand surface, the adhesion was reported to be strengthened by sintering.

Despite the frequent reporting, no mechanisms or a precise and quantitative knowledge of either the coating formation or the bed agglomeration process during the combustion of biomass fuel in fluidized quartz beds have been presented yet. At least 10 different major types of agglomeration mechanisms have been suggested in the literature.[1] For example, the multiple layer illustrations from recent studies showing their existence all seem to be very similar in morphology and characteristics, but the authors draw different conclusions. Both attack or chemical reaction and coating formation by deposition, as well as combinations of the two, have been suggested.

Therefore, the objectives of the present work were to carefully elucidate the bed agglomeration mechanism and main formation processes for the layers of quartz bed particles during the FBC of several typical biomass fuels. Specific goals were (i) to determine if the bed particles are growing outward by deposition, inward by attack/chemical reaction, or a combination of the two; (ii) to determine the characteristics of the formed layers; and (iii) to suggest plausible layer formation and bed agglomeration mechanisms.

Experimental Section

The methodologies used in the present study included the following: (i) bed sampling versus operation time during extended full-scale combustion tests of four different biomass-fired fluidized beds; (ii) bed sampling during controlled bench-scale fluidized-bed agglomeration tests with five representative Nordic biomass fuels selected, with respect to elements

(25) Latva-Somppi, J. *Experimental Studies on Pulp and Paper Mill Sludge Ash Behaviour in Fluidized Bed Combustors*; VTT Publication 336; Technical Research Centre of Finland: Espoo, Finland, 1998; pp 1−89. (Ph.D. Dissertation, Helsinki University of Technology, Helsinki, Finland.)

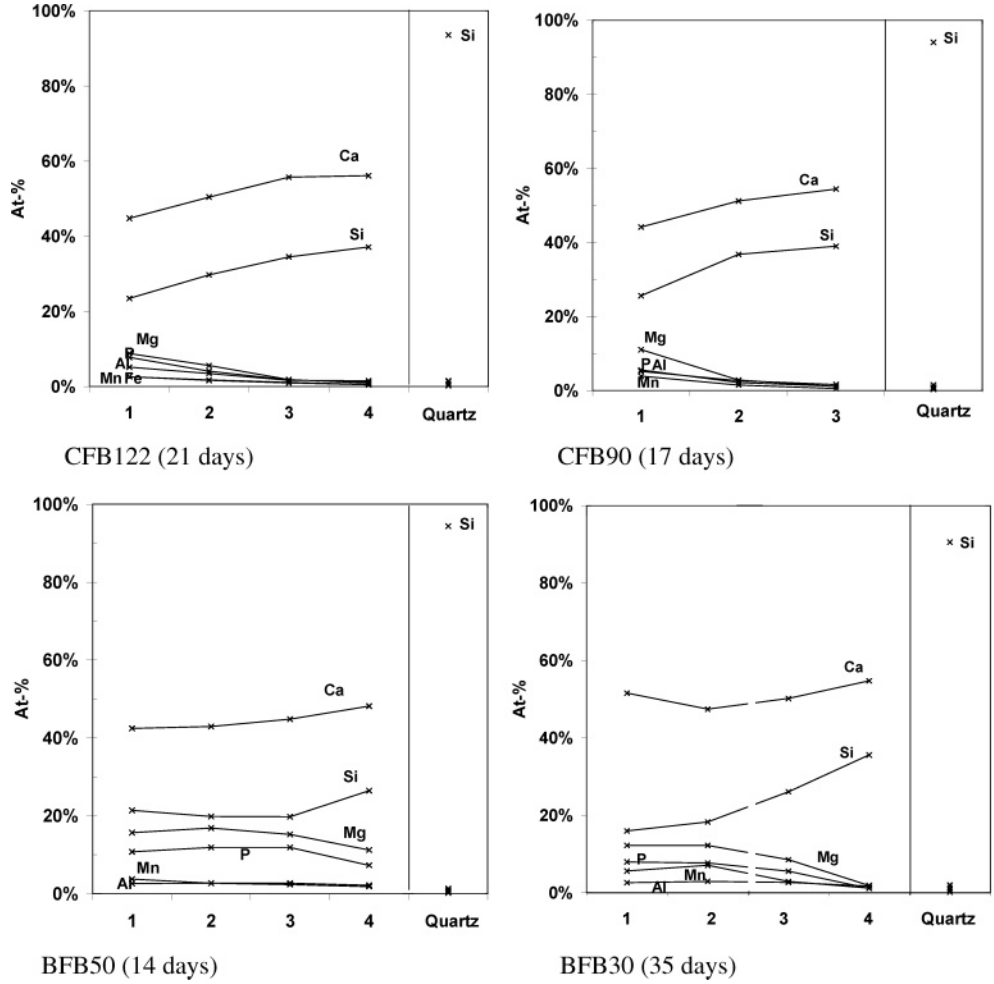

Figure 3. Elemental analyses of the bed material coating following a line from the outside of the outer layer (point 1−3), through the inner layer (point 2−4), and into the surface of the original bed particle.

important for ash formation; and (iii) scanning electron microscopy/energy-dispersive spectroscopy (SEM/EDS) analysis of collected bed material samples, to determine coating characteristics and growth as functions of time from complete bed change.

Full-Scale Experiments. Two different bubbling fluidized bed (BFB) boilers and two circulating fluidized bed (CFB) boilers were included in the study. Typical wood-based fuel mixtures (with an ash composition relatively similar to the bark fuel used in the bench-scale experiments) were used in all plants, which also previously have reported problems related to bed agglomeration. The plants were a 30 MW_{th} BFB (Ahlström) from Falu Energi, a 50 MW_{th} BFB (Foster and Wheeler) from C-4 Energi, a 122 MW_{th} CFB (Foster and Wheeler) from Brista Kraft, and a 90 MW_{th} CFB (Foster and Wheeler) from Skellefteå Kraft (see Table 1 for further details).

Bed material samples (~1 kg) were collected under normal operation conditions from all plants versus operation times of $^1/_2$ h, 1 h, 2 h, 4 h, 8 h, 12 h, and 24 h, as well as 2, 3, 4, ...>14, 35, or 175 days from complete bed change at startup. The same type of fuel was used for the entire sampling campaign in each plant, and the operating conditions were kept as normal and constant as possible. This was verified by logged operation data, as well as semicontinuously determined fuel ash and moisture data. The bed material (>80% quartz) was changed to the same extent as that during normal operation. The reason for the frequent bed changes during normal plant operation is to reduce the risk for bed agglomeration.

Bench-Scale Experiments. Controlled fluidized-bed agglomeration (CFBA) tests were performed with five representative biomass fuels, using quartz sand with a size fraction of 106−125 μm. These relatively small bed particle sizes were chosen to facilitate the determination of the coating/attack-layer thickness of the bed particles.

The raw materials of the five pelletized (6−8 mm) fuels that were used in the experiments were bark, reed canary grass, peat, olive residues, and straw. These materials were selected based on previous work,[14] where principal component analysis (PCA),[26] which is a multivariate data space projection method, was used on a biomass fuel database[27] that contained more than 300 analyzed samples of different biomass fuels, thus covering most of the typical variations in the ash composition of biomass fuels. The fuel characteristics for the five fuels chosen to represent the different classes of biomass fuels in the present study are shown in Table 2.

CFBA tests were conducted using the 5 kW, bench-scale BFB boiler[28] illustrated in Figure 1. The reactor is 2 m high and is composed of stainless steel, with bed and freeboard diameters of 100 and 200 mm, respectively. A perforated stainless-steel distributor plate with 1% open area (90 holes) is used for the fluidizing air.

The fuels were combusted separately, in beds comprised of 540 g of quartz sand, at a bed temperature of 800 °C for 40 h, except for the straw and reed canary grass, which were combusted separately until the bed agglomerated. The fluidization velocity was kept at four times the minimum fluidization velocity of the specific bed material, and the excess oxygen concentration was $6\%_{dry}$ (average), in agreement with a

(26) Wold, S. *Technometrics* **1978**, *20*, 397.
(27) Nordin, A. *Biomass Bioenergy* **1994**, *6*, 339−347.
(28) Öhman, M.; Nordin, A. *Energy Fuels* **1998**, *12*, 90−94.

previously determined standard procedure[28] and typical full-scale conditions.

Bed material samples were collected after different lengths of time from startup (20 min, 40 min, 1 h, 2 h, 4 h, 8 h, 12 h, 16 h, 24, 32, and 40 h). After completed combustion, the bed temperature was increased at a rate of 3 °C/min by means of an external heater in a homogeneous and controlled manner until bed agglomeration was achieved. To avoid the uncertainties associated with the burning particles during this external heating phase, the fuel feeding was turned off and propane precombustion was used to maintain the combustion atmosphere. The maximum possible bed temperature was limited to 1040 °C, because of scaling of the reactor material above this temperature. The onset of bed agglomeration was determined by monitoring differential pressures and temperatures in the bed. The detection of initial bed particle cohesion was facilitated by PCA,[26] considering all bed-related variables (three temperatures and three differential pressures) simultaneously. Earlier results have shown that this method may be used to determine the fuel and bed material specific agglomeration temperature with a reproducibility of ±5 °C (standard deviation, SD).[28] The method has been described in more detail elsewhere.[28]

SEM/EDS Analyses of Bed Material. Bed samples from both full- and bench-scale experiments were mounted in epoxy, cross-sectioned, polished, and analyzed via SEM/EDS. To minimize the effects of noncentral cross sections, and because of the continuous bed change in the full-scale plants during the test campaign, only the largest bed particle cross sections with the thickest layers were analyzed. To specifically determine if the layers are progressing inward or outward, 200 SEM images were taken of both unreacted bed particles and used bed particles after 40 h of bench-scale combustion of olive residue. The images were analyzed to determine cross-sectional areas of original bed particles, full-size areas after 40 h, the combined inner layer and quartz areas, and finally the quartz area after 40 h. To exclude potential significant effects of attrition or thermal stress of bed particles, separate extended runs were performed with propane fuel, where no significant decrease in particle size was observed.

Results and Discussion

Typical illustrations of cross sections of the bed particle surfaces and interfaces between the particles and the layers taken out, versus time from the full-scale plants, are shown in Figure 2. Significant layers of ash-derived compounds developed relatively fast. The initial rate of total layer formation for the bed materials was observed to be relatively high, with a rate of a few micrometers per day, but decreasing to an accumulated layer thickness of up to ~50 μm within 30 days.[9] This accumulated material consisted of two layers. The characteristics of these layers were influenced by both fuel and bed material characteristics. The innermost layers seem to be more homogeneous, consisting of calcium silicates with lower contents of a few other elements. The outer layers seem to more resemble the fuel ash compositions. The transport and layer formation mechanisms, as suggested by Latva-Somppi,[25] seem to explain the structure of all the outer layers obtained in the present work reasonably well, i.e., micrometer-sized particles adhere to the quartz particle surface and subsequently form sintered layers. However, it is, most probably, in combinations with other transport mechanisms such as gas-phase reactions, condensation, and collision with melted ash particles. It could further be noted that some variability in the outer layer composition could be a potential result of variations in the fuel

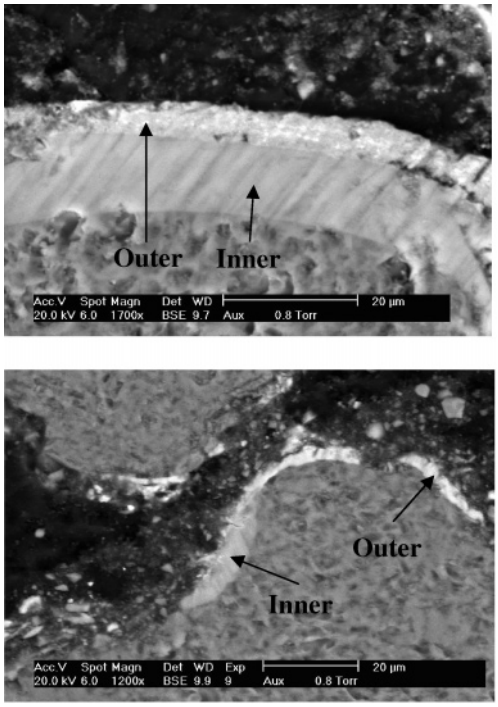

Figure 4. Illustration of typical cross sections of bed particles taken after 40 h of operation in the bench-scale rig during the combustion of olive residue (top) and bark (bottom).

compositions. Extensive EDS spot analysis over the formed layers of several bed particles showed the more homogeneous inner layers to be calcium-enriched, whereas the outer particle-rich layers showed a more complex elemental composition (Figure 3). Because the spatial resolution for accurate quantification using SEM/EDS is a few micrometers, the concentrations presented in Figure 3 could be associated with small uncertainties. For the inner layer compositions, the full-scale results indicate calcium silicates and, to a lesser extent, magnesium silicates, as well as some phosphorus. Both characteristics and total thickness are in general agreement with previous data from the full-scale incineration of waste sludge reported by Latva-Somppi.[25]

For all fuels except straw, significant layers were formed on the bed particles during the CFBA tests. This accumulated material was also determined to consist of two layers (see Figure 4). The samples from the combustion of olive residue and bark in the bench-scale reactor indicate potassium calcium silicates to be the main reaction product. The results from extensive spot analyses made on the layers (Figure 5) showed that the inner layer on the quartz sand consisted mainly of potassium and silicon, with minor amounts of calcium and magnesium, during the combustion of olive residue and potassium, calcium, and silicon during the combustion of bark. The compositions of the outer layers were more complex and were similar to the fuel ash compositions.

The bench-scale effort of trying to determine if the layers are growing inward or outward was successful for the olive fuel, for which sufficiently thick layers were obtained within the 40 h test. The 200 image analyses performed were used to extract the cross-sectional areas of each layer, i.e., the area of the original bed material; the area of the inner layer plus quartz; and also the full

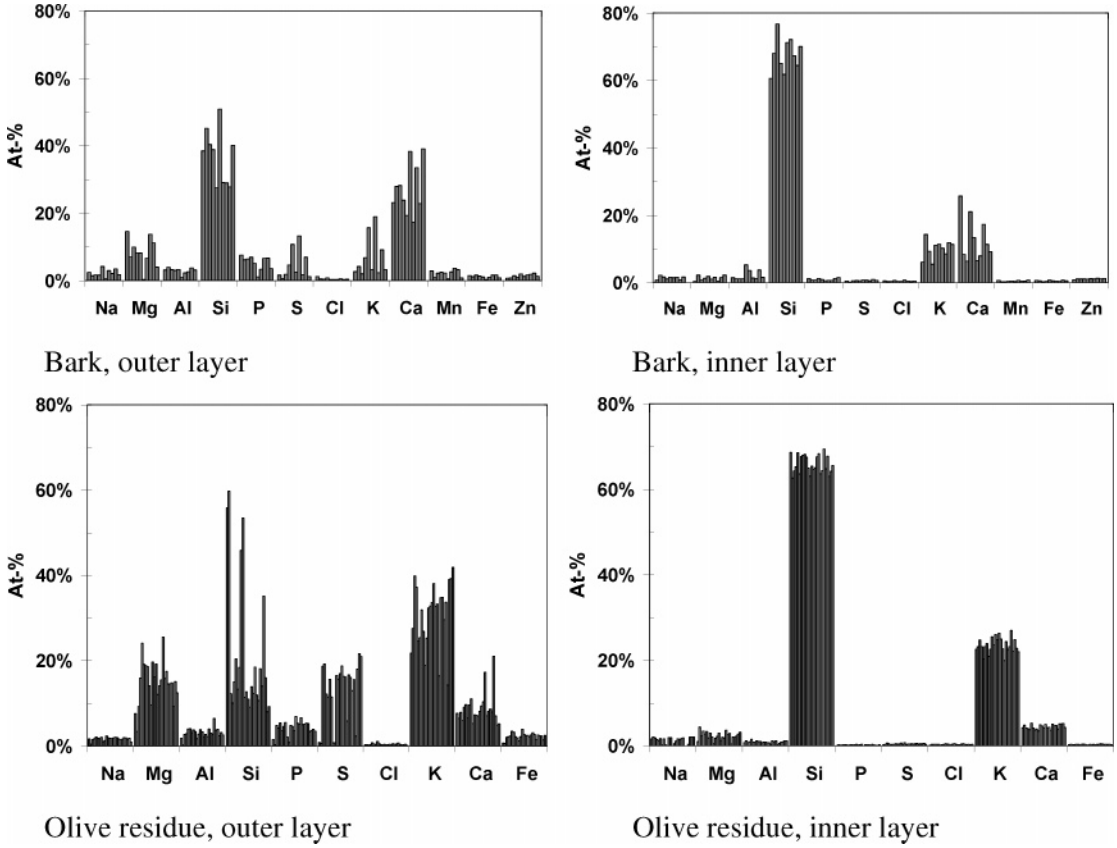

Figure 5. Elemental analyses of the formed layers for bark and olive residue in bench-scale combustion.

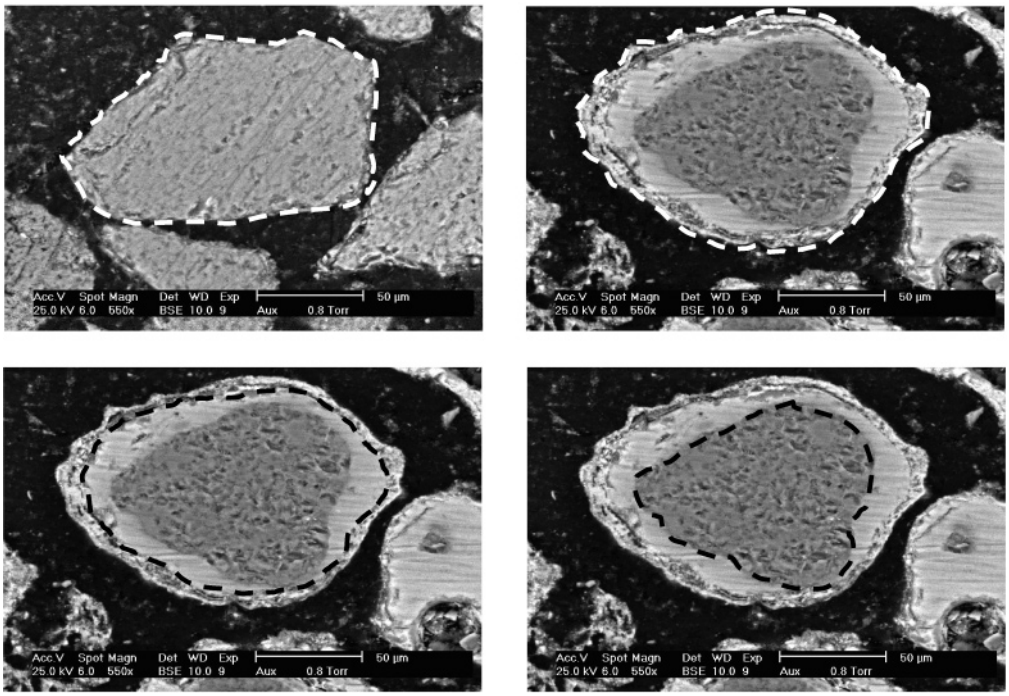

Figure 6. Areas of unreacted bed particles (top left) were measured and compared to the areas of bed particles after 40 h combustion of olive residue (full size (top right), inner layer + quartz (bottom left), and quartz (bottom right)).

size of the layered particles (see Figure 6 for illustrations). For combustion of the olive residue, it could therefore clearly be concluded that the inner layer is mainly growing inward against the interior of the quartz particle i.e., a chemical attack of the original quartz material (Figure 7). Because of the relatively fast and unscheduled bed agglomeration experienced for straw and reed canary grass, and to thin "coating" layers on the bed particles from the bark and peat fuels, the differences in cross-sectional areas between the different layers could not be measured with sufficient accuracy for these fuels. However, although not quantified, strong indications of the same type of attack for the peat and bark fuel was obtained. By careful inspection of the

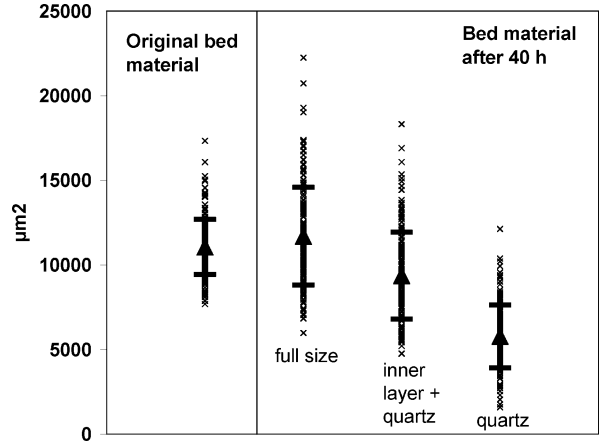

Figure 7. Cross-sectional areas (with mean values and standard deviations) of original bed material and bed material after 40 h of combustion of olive residue.

interfaces between the quartz and the inner layer after a sufficiently long time of burning typical wood fuels in full-scale fluidized beds (Figure 2), it is evident by the irregular reaction front that an inward attack of calcium from the coating is in progress. The reaction is presumably controlled by the diffusion rate of calcium, as also illustrated by the enhanced attack in the vicinity of tension-induced cracks (Figure 2b).

The SEM/EDS analyses of all bed agglomerates from the bench-scale trials showed that either ash-derived silicate melts (straw) or the inner "silicate" layer (olive residue, bark) was responsible for the agglomeration process.[16] Figure 8 shows agglomerates from the combustion of olive residue, bark, and straw. Apparently, the same type of silicate-induced agglomerates was obtained for the straw fuel, with the necks consisting

Table 3. Experimentally Obtained Initial Agglomeration Temperatures: Bench-Scale Experiments

parameter	value
initial agglomeration temp	
bark	990 °C
olive residues	875 °C
peat	>1040 °C
time to agglomeration	
reed canary grass	210 min
straw	65 min

of almost pure potassium silicate, although no coating at all was observed. This indicates agglomeration with direct adhesion by melted ash particles or by burning fuel particles covered by sticky ash.[1] Because of the time scale before agglomeration (65−210 min), compared to the burnout time (minutes) for the fuel particles, the former or a combination of the two seems more likely.

The overall compositional distributions of the melt surrounding the quartz particles are mainly limited (>90%) to different phases of the ternary phase diagram of the $K_2O-CaO-SiO_2$ system. By extracting data from the phase diagram,[29] it was found that the specific agglomeration temperatures, as determined by the CFBA method (see Table 3), agreed fairly well with the temperatures where the melting behavior evaluations indicate high fractions of melt in the silicate layer.

As Valmari[30] showed, these fuels with high reactive silicon and potassium contents result in almost-complete potassium silicate formation and, thus, low-temperature melting particles in the bed. With time, these particles will also most probably continue to be enriched in potassium and, thus, approach even lower melting temperatures and eventually cause sudden severe viscous-flow sintering and agglomeration.

Evidence of a direct attack by gaseous potassium compounds or potassium-containing aerosols was also

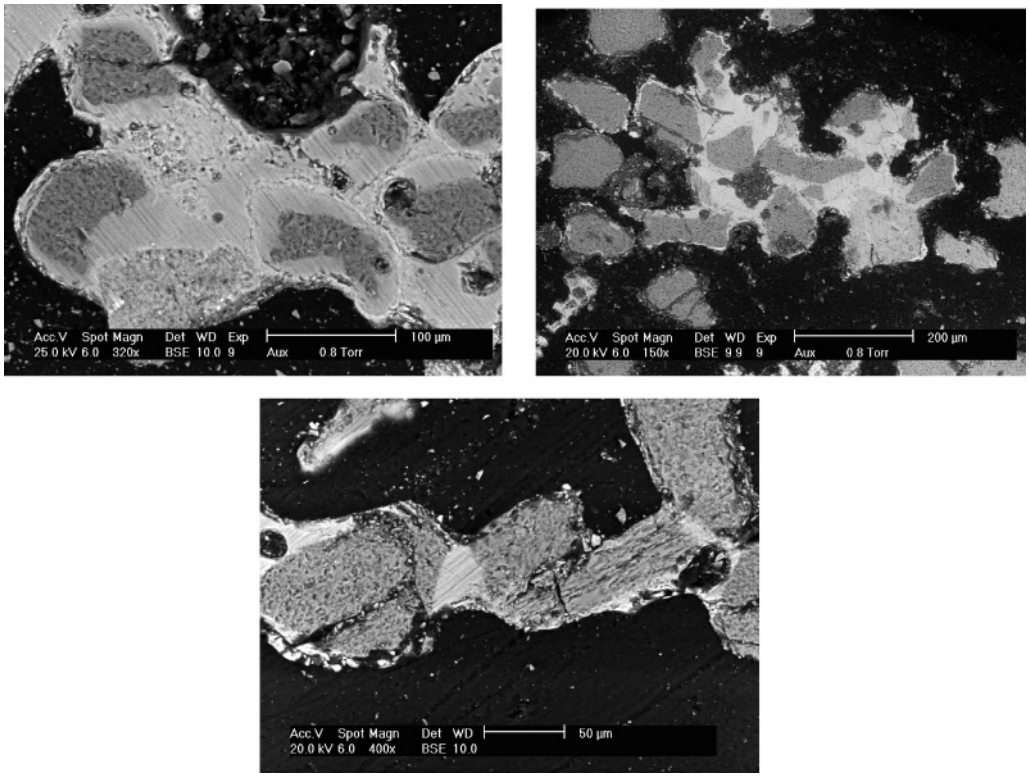

Figure 8. Analyzed agglomerates for olive residues (top left), bark (top right), and straw (bottom) in the bench-scale rig. (From ref 16.)

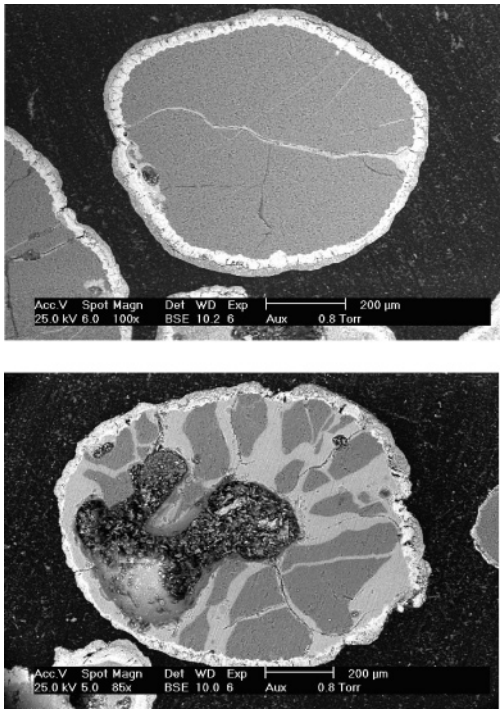

Figure 9. Illustration of typical cross sections of bed particles (quartz) taken after 33 days (top image) and 6 months (bottom image) from the BFB30 plant.

obtained from the samples. The diffusion of potassium in small existing cracks, where other ash compounds could not reach, resulted in the formation of potassium silicate. At typical operational temperatures, this material is partially melted and, thus, allows higher diffusion rates of additional potassium, accelerating a progression and thus continuous widening of the attack and silicate formation. This is nicely illustrated with a typical quartz core of an older (1 and 6 months) quartz particle from the 30 MW BFB plant (Figure 9). All cracks that allow access to only potassium will eventually be surrounded by a wide potassium silicate layer. All the aforementioned results are also in agreement with what could be expected based on thermochemical stability. Calcium silicates are the most stable products and should form from in the interface between ash compounds and quartz. However, if only SiO_2 and potassium compounds are available, potassium silicates will be the most-stable reaction products. However, the rates of formation are controlled by the diffusion conditions.

Conclusions

The following conclusions can be drawn from the present work:

(1) The coating or outer layer formed was determined to be relatively inhomogeneous, consisting of small particles that resemble the fuel ash compositions. However, in addition to small particles adhering to the quartz, the formation may also include gas-phase reactions, condensation, and collision with melted ash particles.

(2) The inner layers observed were all found to grow inward by an attack or chemical reaction with the quartz in the bed particles, forming calcium-dominated silicates directly under the ash-derived outer layer, and potassium or alkali silicates wherever other ash-forming elements are less available, i.e., in cracks and for high-potassium- and sodium-containing fuels.

(3) As has been previously well-established, melt formation is a dominating mechanism in bed agglomeration.

(4) Of the previously suggested agglomeration mechanisms, a few have now been identified to be dominating for biomass fuels, including the following: (a) coating-induced agglomeration with the subsequent attack and diffusion by calcium into the quartz, forming low-melting silicates (also including minor amounts of, for example, potassium) with subsequent viscous-flow sintering and agglomeration (for typical wood fuels); (b) direct attack by potassium compounds in the gas or aerosol phase, forming low-melting potassium silicate with subsequent viscous-flow sintering and agglomeration (for high alkali-containing biomass fuels); and (c) direct adhesion by partly melted ash-derived potassium silicate particles/droplets (for fuels containing both potassium and reactive silicon but a lesser extent of other ash-forming elements).

Acknowledgment. The financial support from the Swedish Energy Agency and the Thermal Engineering Research Foundation (Värmeforsk) is gratefully acknowledged. Assistance from the operating personnel at Brista Kraft, C-4 Energi, Falu Energi, and Skellefteå Kraft is greatly appreciated.

EF0400868

(29) Morey, G. W.; Kracek, F. C.; Bowen, N. L. *J. Soc. Glass Technol.* **1930**, *14*, 158.

(30) Valmari, T. *Potassium Behaviour during Combustion of Wood in Circulating Fluidized Bed Power Plants*; VTT Publication 414; Technical Research Centre of Finland: Espoo, Finland, 2000; pp 1−88. (Ph.D. Dissertation.)